I&EC research
Industrial & Engineering Chemistry Research

Article

Cite This: Ind. Eng. Chem. Res. 2018, 57, 7795−7801

pubs.acs.org/IECR

Chlorine Production by HCl Oxidation in a Molten Chloride Salt Catalyst

Shizhao Su,[†] Davide Mannini,[‡] Horia Metiu,[‡] Michael J. Gordon,[†] and Eric W. McFarland*[,†]

[†]Department of Chemical Engineering, University of California, Santa Barbara, California 93106-5080, United States
[‡]Department of Chemistry and Biochemistry, University of California, Santa Barbara, California 93106-9510, United States

ABSTRACT: A molten salt mixture containing 45 mol % KCl and 55 mol % $CuCl_2$ was investigated as a catalyst for the reaction of HCl with O_2 to produce Cl_2. The HCl conversion for an HCl:O_2 molar feed ratio of 1:2 at 450 °C and a total pressure of 1 atm was 80% at a residence time of less than 1 s in a lab scale bubble column reactor. The equilibrium conversion at this temperature and pressure is 84%. The catalyst system was found to remain stable throughout a continuous 24-h experiment. The use of a mixed transition metal/alkali metal molten salt catalyst for HCl oxidation reduces the volatility of supported chlorides and may avoid the mechanical stability limitations of solid catalysts caused by volume changes between the halide and the oxide.

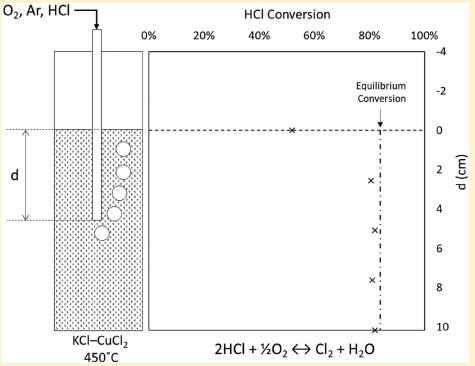

1. INTRODUCTION

Chlorine is a vital commodity chemical for the global economy. The worldwide demand for chlorine in 2015 was 71 million tons and is expected to exceed 100 million tons by 2024.[1] Chlorine (Cl_2) is produced predominantly by the electrochemical chlor-alkali process.[2−5] Most chlorine is used for the production of vinyl chloride monomer (VCM), polyvinyl chloride (PVC), isocyanates, and oxygenates (e.g., propylene oxide and propane-1,3-diol). Hydrogen chloride (HCl) is a common byproduct of chlorine use, and there is significant interest in cost-effective methods to recover Cl_2 from HCl.

Although electrochemical processes are used today, direct catalytic oxidation of HCl with oxygen to produce Cl_2 and water was first developed in the late 1800s using solid CuO/$CuCl_2$ catalyst[6,7] and is known as the Deacon process. The reaction is exothermic and equilibrium limited in practice. Separation of the final products and reactor heat transfer are challenging and add to the process cost. In attempts to reduce reaction temperatures, several catalysts have been developed and tested in semicommercial processes, namely, SiO_2 supported copper-didymium-potassium chloride (Shell Chlorine Process),[8−11] Cr_2O_3/SiO_2 catalyst (Mitsui Process),[12,13] and rutile oxide (RuO_2) (Sumitomo Process).[14−20] Catalyst volatilization is the main cause of deactivation for chloride-based catalysts,[21] while volume change associated with the solid oxide to chloride conversion are thought to contribute to deactivation.[22,23] Figure 1 shows the process flowsheet of the state-of-the-art Sumitomo HCl oxidation process using a fixed bed tube reactor and RuO_2/rutile TiO_2 as catalyst. The product has to go through multiple separation steps to obtain pure Cl_2 and recycle unreacted O_2 and HCl.[24]

If limitations in catalyst lifetime and reactor heat transfer were reduced, catalytic HCl oxidation might be cost competitive with electrochemical chlorine production. We investigated molten chloride salts as catalysts for HCl oxidation. Whereas the solid catalyst undergoes continuous cyclic conversion between the solid halide and solid oxide, each with different unit cell volumes thought to promote mechanical degradation, the melt eliminates the structural fatigue and provides a continuously renewed gas−liquid interface with effectively unlimited lifetime. Further, molten salts have excellent heat transfer properties, avoiding "hot spots", and when relatively volatile molten transition metal halide salts are mixed with alkali metal halides, the volatility of the transition metal halide is decreased. Molten halide salts have been used as catalysts in a number of chemical processes,[25,26] and the unit operations and system management are well understood. Molten salt catalysts have been used in extraction of ores,[27] metal production,[28−32] catalytic coal gasification,[33] Wacker oxidation of ethylene,[34] diesel soot catalytic oxidation,[35] and oxidative dehydrogenation of alkanes.[25,26,36]

For HCl oxidation, the Deacon reaction mechanism over $CuCl_2$ has been previously described[10,37−39] as

$$2CuCl_2 \rightleftarrows 2CuCl + Cl_2 \quad (1)$$

$$2CuCl + \frac{1}{2}O_2 \rightarrow CuO + CuCl_2 \quad (2)$$

$$CuO + 2HCl \rightarrow CuCl_2 + H_2O \quad (3)$$

Combining reactions 1−3 gives the overall reaction:

Received: March 15, 2018
Revised: May 14, 2018
Accepted: May 22, 2018
Published: May 22, 2018

DOI: 10.1021/acs.iecr.8b01141
Ind. Eng. Chem. Res. 2018, 57, 7795−7801

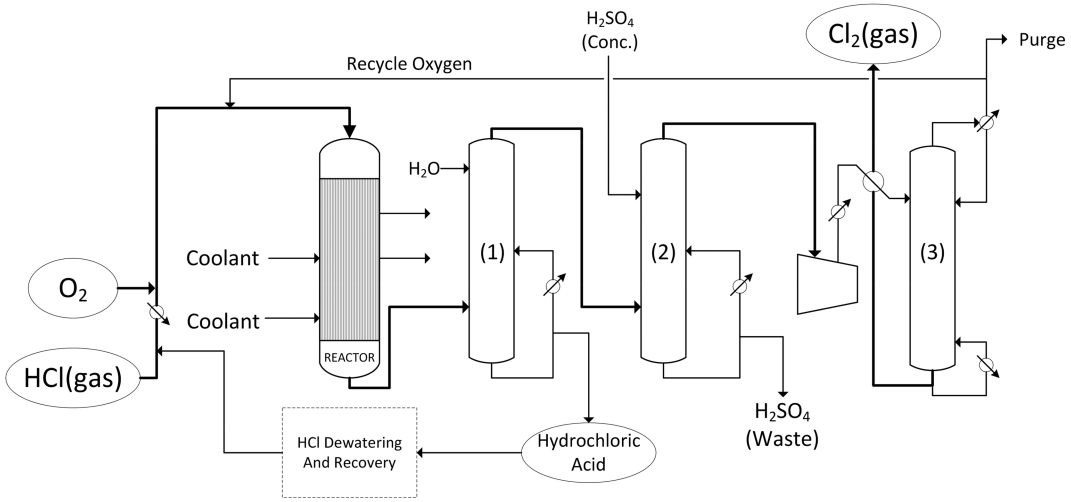

Figure 1. Flowsheet of the Sumitomo HCl oxidation process in a fixed bed tube reactor using RuO_2/rutile TiO_2 as catalyst.[24] The product mixture goes through multiple separation steps to obtain pure Cl_2 product: (1) HCl absorption, (2) drying, and (3) O_2/Cl_2 separation.

$$2HCl + \frac{1}{2}O_2 \rightleftarrows Cl_2 + H_2O \quad (4)$$

The free energy change, ΔG^0, as a function of temperature for the equilibrium-limited reaction is shown in Figure 2 for

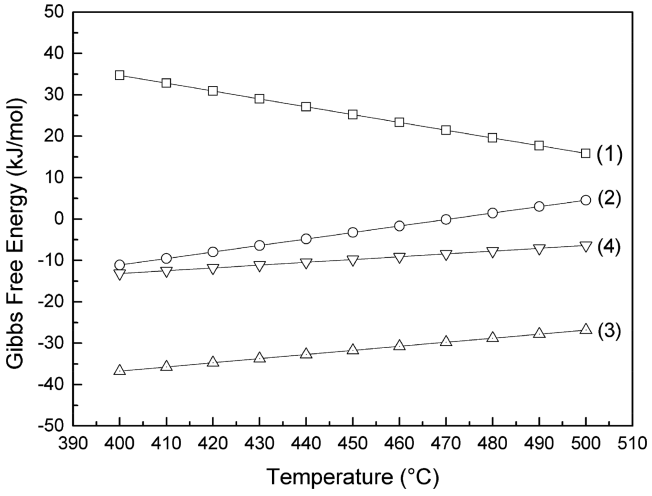

Figure 2. Gibbs free energy changes, ΔG^0, of reaction 1, $2CuCl_2 \leftrightarrow 2CuCl + Cl_2$; 2, $2CuCl + {}^1/_2O_2 \rightarrow CuO + CuCl_2$; 3, $CuO + 2HCl \rightarrow CuCl_2 + H_2O$; and the overall reaction 4, $2HCl + {}^1/_2O_2 \leftrightarrow Cl_2 + H_2O$ as a function of reaction temperature. Values calculated using HSC chemistry software (Outotec Research Oy, Finland).[41]

reactions 1−4. ΔG^0 for reaction 1 is positive and large. However, reaction 2 consumes CuCl and shifts the equilibrium of reaction 1 toward the products. In addition, reaction 3 favorably shifts the equilibrium of reaction 2.

It is believed that the reaction rates are such that $CuCl_2$ is in thermodynamic equilibrium with CuCl and Cl_2, even when the overall reaction is run at steady state.[9] It is noteworthy that the detailed reaction mechanism is more complicated than reactions 1−3. The oxychloride (Cu_2OCl_2), and hydroxyoxichlorides ($Cu(OH)Cl$, $Cu_2(OH)_3Cl$) may be important reaction intermediates.[40]

The original work with supported copper chloride catalysts was limited by the volatility of the chloride, heat management, and degradation of the supported catalyst due to cyclic volumetric stresses. In this article, we address the following questions: (1) Can a mixture of copper chloride and potassium chloride provide stable activity in a molten state for HCl oxidation? (2) How does the reaction activity and stability of the molten salt change as a function of the HCl/O_2 feed ratio? (3) In a lab-scale bubble column, how does conversion vary with the height of the bubble column? (4) How to characterize the catalytic reaction by measuring the HCl conversion as a function of time and/or residence time at different temperatures and feed concentration?

2. EXPERIMENTAL METHODS

2.1. Reactor System. Molten salts were contacted with gas phase reactants in a small bubble column reactor consisting of a quartz tube sealed at the bottom with a diameter of 0.88 cm and length of 20 cm. Reagent grade (≥99%) anhydrous potassium chloride (KCl) used in the experiments was from Honeywell Fluka Chemicals. Analytical reagent grade (≥99.8%) cupric chloride ($CuCl_2{\cdot}2H_2O$) used in the experiments was from Mallinckrodt. The cupric chloride was dried in a box furnace at 120 °C[42−45] overnight (>12 h) to produce anhydrous $CuCl_2$. Fifteen grams of powdered anhydrous salt (45 mol % KCl−55 mol % $CuCl_2$) was loaded in the reactor and heated above 400 °C in a tubular ceramic fiber heater (Watlow) to form a liquid. The experiments were operated in a fume hood to avoid any potential safety hazards caused by HCl and Cl_2 gas. According to the binary phase diagram of KCl−$CuCl_2$[46] the liquidus temperature of the salt mixture is lower than 365 °C. The liquid height in the reactor was 10.5 cm. To ensure that the salt was dehydrated, argon was sparged through the melt for 30 min. The reactant feed stream containing HCl and O_2 was prepared by bubbling a mixture of Ar and O_2 through concentrated hydrochloric acid via a Pyrex gas sparger. The mixed gas flow rate of Ar and O_2 was set to 20 sccm. The total pressure of the reactant feed stream was 1 atm at all times. Trace amounts of H_2O vapor (<0.5 sccm) were introduced in the gas feed due to the vaporization of H_2O from the hydrochloric acid. A chloride ion selective electrode (ISE) probe (Cole-Parmer, United States) measured the HCl flow rate prior to the reaction. The gas phase reactants (Ar, HCl, and O_2) were introduced into the bubble column through a quartz tube with an inside diameter of 1 mm as shown in Figure

DOI: 10.1021/acs.iecr.8b01141
Ind. Eng. Chem. Res. 2018, 57, 7795−7801

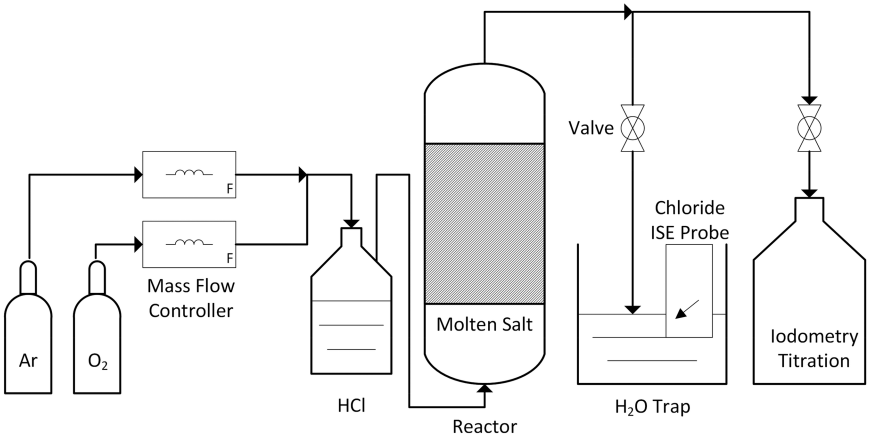

Figure 3. Schematic of the experiment setup. The reactor consists of a quartz tube sealed at the bottom with a diameter of 0.88 cm and length of 20 cm. The liquid height of molten salt (45 mol % KCl−55 mol % $CuCl_2$) in the reactor was 10.5 cm. The quartz inlet tube had an inner diameter of 1 mm and was inserted to the bottom of the molten salt to deliver a gas mixture of O_2, Ar, and HCl.

3. The reactor effluent, a mixture of Cl_2, H_2O, unreacted HCl and O_2, was passed through a potassium iodide (KI) solution. The Cl_2 in the effluent reacts with KI and forms I_2. The amount of I_2 in the solution was titrated with a standard NaS_2O_3 solution. The iodometric titration result was used to determine the Cl_2 production rate. The Cl_2 production was attributed to the HCl feed and used to calculate the apparent HCl conversion. The chloride ISE probe was also used to measure the total amount of Cl_2 and unreacted HCl in the reactor effluent. The total amount of chlorine in the reactor effluent was compared with that in the influent to ensure that all Cl_2 generated during the reaction comes from the HCl feed, and the molten salt catalyst was not consumed.

2.2. Reactant Composition Dependent Activity. The effect of gas composition on HCl conversion was investigated over a range of molar feed ratios. At a reaction temperature of 450 °C, the molar ratio of HCl to oxygen (n(HCl)/n(O_2)) in the feed was varied from 2:1 to 1:3, as shown in Table 1.

Table 1. Reactant Gas Molar Ratios and Flow Rates for Activity Measurements

n(HCl):n(O_2)	HCl flow rate (sccm)	O_2 flow rate (sccm)	Ar flow rate (sccm)
2:1	5.0	2.5	17.5
1:1	3.0	3.0	17.0
1:2	4.8	9.6	11.4
1:3	2.5	7.5	12.5

2.3. Temperature and Residence Time Dependency and Stability. The dependence of HCl conversion on bubble residence time in the column was measured by changing the immersion depth of the gas inlet tube in the molten salt. The gas residence time is approximately proportional to the effective bubble column length, which is determined by the distance between the surface of the molten salt and the end of the gas inlet tube. The flow rates of HCl, O_2, and Ar were 2.5, 5, and 15 sccm, respectively. The HCl conversion was measured at 400 and 450 °C. The bubble size and bubble rise velocity was directly measured with a video camera by passing argon bubbles through a 2 mm ID quartz inlet tube in a molten 50 mol % KCl−50 mol % $ZnCl_2$ salt at 450 °C. The KCl−$ZnCl_2$ molten salt has similar physical properties with the KCl−$CuCl_2$ salt. The density of equimolar KCl−$ZnCl_2$ molten salt[47] is 2.150 g/cm^3, and the density of equimolar KCl−$CuCl_2$ molten salt[48] is 2.225 g/cm^3. It is easier to characterize the bubble in molten KCl−$ZnCl_2$ because it was colorless and transparent, while molten KCl−$CuCl_2$ was black. The bubble rise velocity was approximately 17 cm/sec, and the bubbles were approximately 5 mm in diameter.

The activity was measured at 450 °C over a 24-h period of continuous operation with flow rates of HCl, O_2, and Ar of 6.9, 9.7, and 10.3 sccm, respectively. The HCl conversion was measured as a function of time on stream.

3. RESULTS AND DISCUSSION

3.1. Dependence of Activity on Reactant Composition. The stable operation of the bubble column reactor relies on the complete regeneration of $CuCl_2$ in reaction 3. Hence, it is crucial to ensure that the rate of reaction 3 is faster than that of reaction 4 so that the process is not going to be limited by the HCl feed. Under such conditions, all Cl_2 produced can be attributed to the HCl feed. On the other hand, when oxidation reaction 4 is faster than reaction 3, part of the Cl_2 produced must be attributed to the net reaction between $CuCl_2$ and O_2. This means that some of the CuO is not completely converted to $CuCl_2$ by the HCl feed.

Here, we define the ratio x as the Cl_2 production rate with respect to the HCl feed ($x = 2n(Cl_2)/n(HCl)$). Under the reaction conditions where CuO is completely converted to $CuCl_2$, the ratio x is effectively the HCl conversion. The HCl conversion x for different HCl/O_2 molar ratios is shown in Figure 4. For each HCl/O_2 molar ratio, the apparent HCl conversion increases with time and then levels off. During the reaction, it is likely that the reaction intermediate CuO is formed in the melt and rises to a steady-state level. According to reaction 3, CuO is the active species in the melt that reacts with HCl. The continuous formation of CuO increases the apparent HCl conversion x. The composition of the melt gradually reaches steady state with time on stream. This leads to the eventual stabilization of the apparent HCl conversion x. An exception to this trend occurs when the HCl/O_2 molar ratio is 1:3, when the apparent HCl conversion increases to 98% and then decreases gradually. The initial increase of the apparent HCl conversion x is due to the formation of CuO, following the same reaction scheme with other experiments where the HCl/O_2 ratios are higher than 1:3. As the reaction proceeds, the

DOI: 10.1021/acs.iecr.8b01141
Ind. Eng. Chem. Res. 2018, 57, 7795−7801

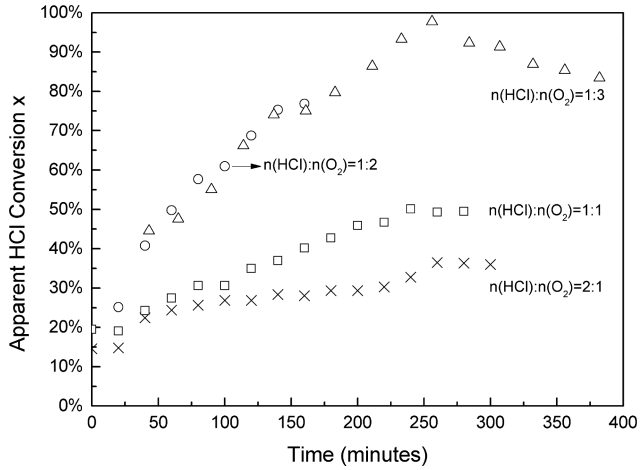

Figure 4. Apparent HCl conversion for various HCl/O_2 feed molar ratios at 450 °C. The molten salt had a height of 11 cm. The total reactant flow rate was approximately 24 sccm (as shown in Table 1).

excessive O_2 in the gas feed favors reaction 2 and irreversibly converts the CuCl in the melt to CuO. As CuO accumulates in the melt, the molar activity of $CuCl_2$ continuously decreases in the melt, causing the decrease of apparent HCl conversion x.

To validate this hypothesis, the chlorine balance was examined for each HCl/O_2 molar ratio in separate experiments when the apparent HCl conversion was stable. The feed gas compositions and flow rates are shown in Table 2. As described

Table 2. Reactant Gas Molar Ratios and Flow Rates in the Chlorine Balance Experiment

$n(HCl):n(O_2)$	HCl flow rate (sccm)	O_2 flow rate (sccm)	Ar flow rate (sccm)
2:1	6.9	3.5	16.5
1:1	2.8	2.8	17.2
1:2	1.8	3.6	16.4
1:3	2.1	6.3	13.7

in the Experimental Section, the Cl_2 and unreacted HCl were measured with the chloride ISE probe. Then, the amount of total chlorine in the effluent was compared with the amount of chlorine in the HCl feed. The results shown in Figure 5 are

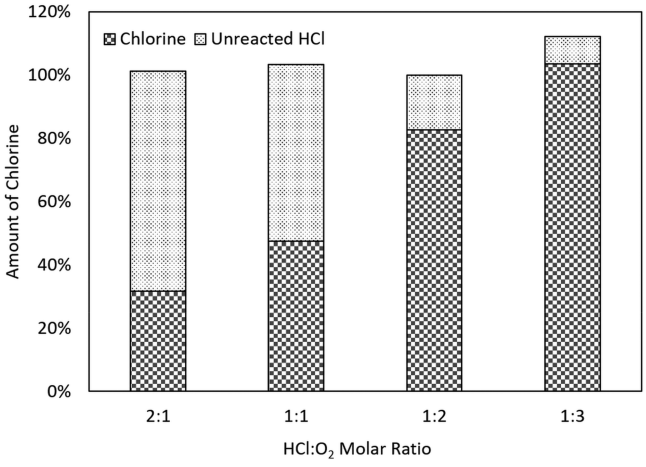

Figure 5. Chlorine mass balance closure in the reactor effluent with various HCl/O_2 feed molar ratios (shown in Table 2) at 450 °C.

based on integrated data over 20 min of reaction time after the apparent HCl conversion x reached steady state, except for an HCl/O_2 feed ratio of 1:3 where, as mentioned in Section 3.1, the apparent HCl conversion x did not reach a steady state when the HCl/O_2 feed ratio was 1:3. The result in Figure 5 when the HCl/O_2 feed ratio was 1:3 was based on integrated data of unreacted HCl and the Cl_2 product over 20 min of reaction time when the apparent HCl conversion x was the highest (~98%). When the HCl/O_2 molar ratio was between 2:1 and 1:2, the total amount of chlorine entering the reactor was equal to the amount exiting the reactor. For these ratios, all chlorine produced originated from the HCl feed; the apparent HCl conversion x is equal to the real HCl conversion. When the HCl/O_2 molar ratio was 1:3, the total amount of chlorine (in HCl or Cl_2) exiting the reactor exceeded the amount of chlorine in the HCl feed. This indicates that some of the $CuCl_2$ was irreversibly converted to CuO. It is obvious that the accumulation of CuO should be avoided to prolong catalyst lifetime. Therefore, the optimal HCl/O_2 molar ratio for our bubble column reactor at 450 °C was 1:2.

3.2. Temperature and Residence Time Dependence. When the HCl/O_2 feed molar ratio was 1:2, all Cl_2 from the effluent originate from HCl. The HCl conversion as a function of bubble column length for this HCl/O_2 ratio of 1:2 is shown in Figure 6. Each data point in Figure 6 represents the steady

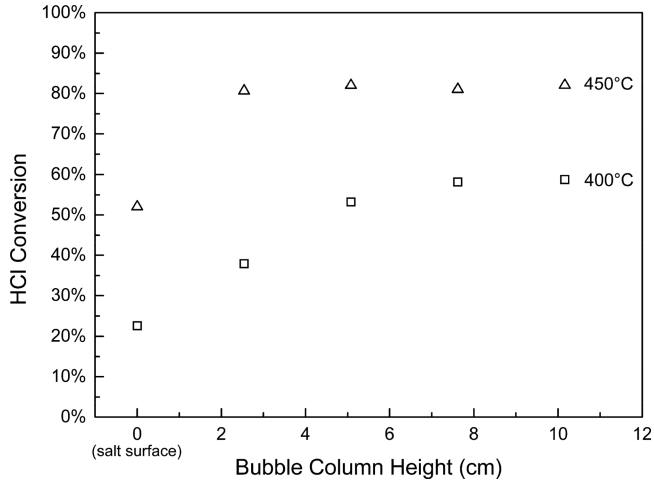

Figure 6. HCl conversion with various bubble column heights at 400 and 450 °C with HCl/O_2 feed ratio of 1:2.

state HCl conversion as a function of bubble column height at temperature. The HCl conversion at zero column height was due to the reaction at the molten salt surface, i.e. the tube through which the feed was inserted in the reactor was not immersed in the melt but the gas came in contact with the surface.

The calculated equilibrium HCl conversion for reaction 4 at 450 °C when HCl/O_2 = 2:1 is 84%. In our measurements, the HCl conversion soon reaches 81% at 8 cm, which is close to equilibrium.

At 400 °C, the HCl conversion slowly increases from 22%, when the gas is in contact to the surface (the tube is not immersed in the melt), to 59%, when the gas bubbles through a 10 cm high column of melt. The HCl conversion at 400 °C is lower than that of 450 °C, even though the thermodynamics of reaction 4 favor low temperature (ΔG = −13.1 kJ/mol at 400 °C). Based on the thermodynamics (Figure 2), the

DOI: 10.1021/acs.iecr.8b01141
Ind. Eng. Chem. Res. 2018, 57, 7795−7801

decomposition of $CuCl_2$ (reaction 1) is unfavorable at low temperatures. Although the reaction between CuCl and O_2 (reaction 2) would continuously pull the equilibrium of reaction 1 toward the product, previous research has shown that the reaction rate between O_2 and molten halide salts decreases at low temperatures.[25,26] It is likely that when the bubble column height is larger than 8 cm, the reaction rate is limited by the thermodynamic equilibrium of reaction 1 and the reaction kinetics of reaction 2. Therefore, it is beneficial to operate the HCl oxidation process in the molten KCl−$CuCl_2$ catalyst at 450 °C. An alternative is to search for catalysts that would increase the rate, so one can operate at lower temperature. Possible approaches include adding a rare earth chloride to the melt[8,49] or introducing soluble oxides in the melt system to avoid diffusion-limited mass transfer. The results presented here by no means optimized in terms of reactor design variables to minimize mass transfer limitations of rate; bubble size and bubble column hold-up can be further investigated to minimize the mass transfer limitations and maximize the overall rate for potential industrial applications.

3.3. Stability of the Molten Salt Catalyst System. For an HCl:O_2 feed ration of 1:1.4, all chlorine product originates from the conversion of HCl. For this reason, we selected these conditions to investigate the stability of the system. Figure 7

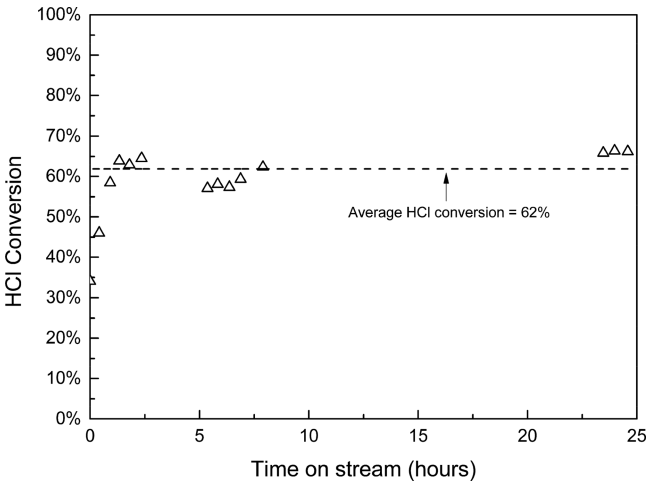

Figure 7. Molten salt stability study at 450 °C with HCl/O_2 feed ratio of 1:1.4.

shows that the steady-state performance was constant for 24 h. The graph also shows that it takes about 1 h for the system to reach steady state. The amount of Cl_2 produced during the 25 h experiment was calculated to be 0.125 mol. The total quantity of $CuCl_2$ in the bubble column was 0.071 mol. The turnover number over the course of the reaction is 1.75, and there was no observed decrease in rate. There is no evidence that the $CuCl_2$ is consumed or loses activity as a catalyst.

3.4. Analysis of the Cooled Catalyst. Figure 8 shows the X-ray diffraction (XRD) spectra of two salt samples after cooling and solidification. The top spectrum is that of a quenched molten KCl−$CuCl_2$ that contained 45 mol % KCl and 55 mol % $CuCl_2$. The bottom spectrum is taken from quenched molten KCl−$CuCl_2$ salt after having been used to perform the HCl oxidation reaction for 24 h. Both quenched salt samples contain three species: $KCuCl_3$, $K_4Cu_4OCl_{10}$, and CuO. Based on the phase diagram of the KCl−$CuCl_2$ system[46] and previous research on $K_4Cu_4OCl_{10}$, also known as

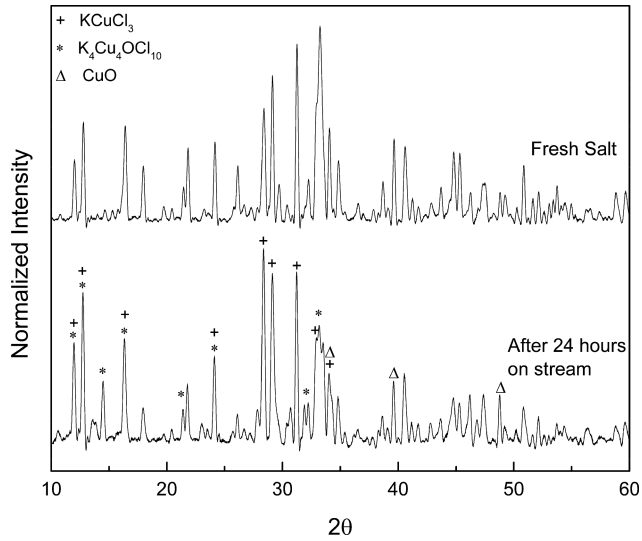

Figure 8. XRD spectra of quenched molten salt catalysts in fresh state (top spectra) and after 24 h on stream of HCl oxidation reaction (bottom spectra). The characteristic peaks of $KCuCl_3$, $K_4Cu_4OCl_{10}$, and CuO are shown as + , *, and Δ, respectively.

Ponomarevite,[50] we speculate that $KCuCl_3$ and $K_4Cu_4OCl_{10}$ were formed during cooling of the molten salt. Although the cooled salt does not reflect the active sites in the molten salt during the reaction, the elemental composition of the cooled salt represents the molten state. XRD shows there is more $K_4Cu_4OCl_{10}$ and CuO in the solid sample of the salt after 24 h of HCl oxidation. The formation of $K_4Cu_4OCl_{10}$ and CuO suggest that during HCl oxidation, copper oxide or copper oxychloride is formed in the molten salt. The equilibrium composition of the molten salt depends on the equilibrium of reactions 1−3. CuCl was not detected in either of the quenched samples.

A sample of molten KCl−$CuCl_2$ salt, which was used in the HCl oxidation reaction for 24 h, was quenched and then dissolved in water. A 55 mm diameter Whatman filter paper No. 41 (20−25 μm pore size) was used to remove the water-soluble KCl and $CuCl_2$. The remaining solid was dried at 90 °C in an oven for 12 h and characterized by scanning electron microscopy (SEM)/energy-dispersive X-ray spectroscopy (EDS) analysis. The result is shown in Figure 9. The EDS spectra show that the extract consists of oxygen, chlorine, and copper. Copper oxide and water insoluble copper oxychloride formed during quenching of the molten salt. This characterization proved the existence of CuO or copper oxychloride in the liquid molten KCl−$CuCl_2$ salt during the HCl oxidation process. The CuO and copper oxychloride is very likely to form solid particles that are dispersed in the molten salt and form a slurry. A sample of quenched molten KCl−$CuCl_2$ salt was also dissolved in water and filtered with Whatman filter paper. No solid remains was detected from the filter paper.

4. SUMMARY AND CONCLUSIONS

The addition of potassium chloride to copper chloride provides a mixture that is molten at reaction temperatures and is an active catalyst for HCl oxidation to produce Cl_2 from H_2O. The molten catalyst eliminates mechanical catalyst degradation caused by solid halide-to-solid oxide conversion, and the presence of the alkali chloride reduces the copper chloride volatility. At 450 °C and 1 atm of total pressure, 81% HCl

DOI: 10.1021/acs.iecr.8b01141
Ind. Eng. Chem. Res. 2018, 57, 7795−7801

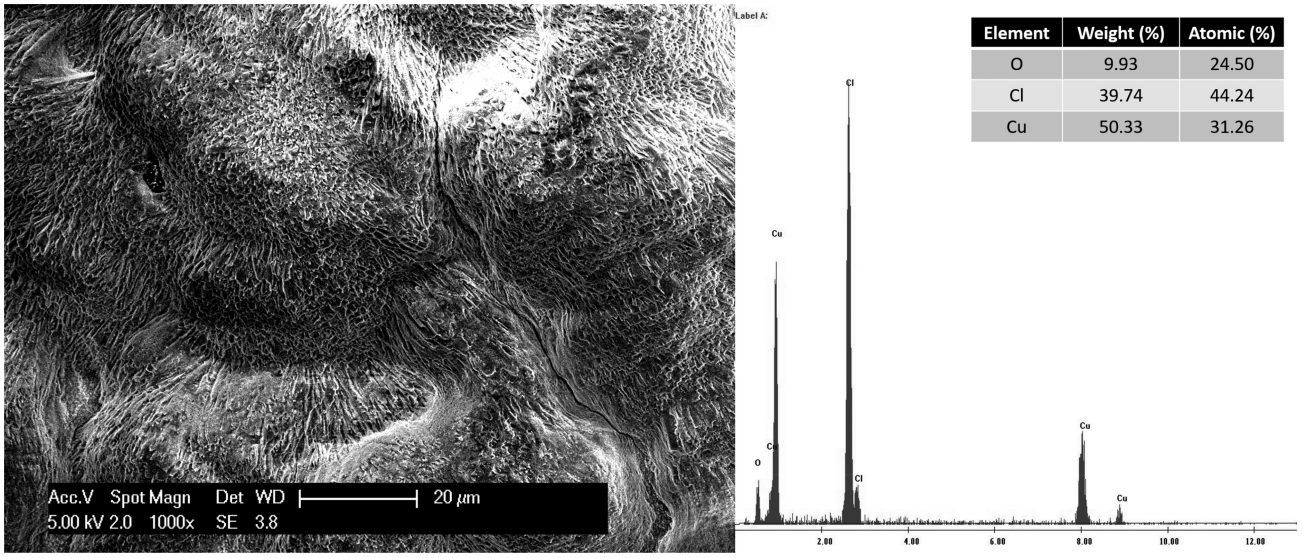

Element	Weight (%)	Atomic (%)
O	9.93	24.50
Cl	39.74	44.24
Cu	50.33	31.26

Figure 9. SEM image and EDS spectra of the quenched KCl−$CuCl_2$ molten salt after 24 h of catalyst stability testing. The EDS spectra were taken from the full area of the SEM image.

conversion was achieved for an HCl:O_2 molar feed ratio of 1:2 in a 11 cm laboratory scale bubble column with residence time less than 1 s. The molten catalyst showed no activity change during an uninterrupted, 24-h run. With such high activity, a molten-salt catalyst configured in a bubble column has potential for industrial catalytic production of Cl_2 by direct oxidation of HCl.

AUTHOR INFORMATION

Corresponding Author

*E-mail: ewmcfar@engineering.ucsb.edu.

ORCID

Shizhao Su: 0000-0002-0697-4207

Horia Metiu: 0000-0002-3134-4493

Notes

The authors declare no competing financial interest.

ACKNOWLEDGMENTS

This work was supported by BASF through the California Research Alliance Program (CARA) with partial support from the U.S. Department of Energy, Office of Science, Office of Basic Energy Sciences Grant DE-FG03-89ER14048. The authors acknowledge the technical assistance of Mr. Steven Bustillos.

REFERENCES

(1) Grand View Research. *Chlorine Market Analysis By Application (EDC/PVC, Organic Chemicals, Inorganic Chemicals, Isocyanates, Chlorinated Intermediates, Propylene Oxide, Pulp & Paper, C1/C2 Aromatics, Water Treatment) And Segment Forecast To 2024*; Grand View Research: San Francisco, CA, 2016.

(2) Moussallem, I.; Jorissen, J.; Kunz, U.; Pinnow, S.; Turek, T. Chlor-Alkali Electrolysis with Oxygen Depolarized Cathodes: History, Present Status and Future Prospects. *J. Appl. Electrochem.* **2008**, *38* (9), 1177−1194.

(3) Hine, F.; Nozaki, M.; Kurata, Y. Bench Scale Experiment of Recovery of Chlorine from Waste Gas. *J. Electrochem. Soc.* **1984**, *131* (12), 2834.

(4) Motupally, S.; Mah, D. T.; Freire, F. J.; Weidner, J. W. Recycling Chlorine from Hydrogen Chloride- a New and Economical Electrolytic Process. *Electrochem. Soc. Interface* **1998**, *7* (3), 32−36.

(5) Allen, R. J.; Giallombardo, J. R.; Czerwiec, D.; De Castro, E. S.; Shaikh, K.; Gestermann, F.; Pinter, H. D.; Speer, G. Process for the Electrolysis of Technical-Grade Hydrochloric Acid Contaminated with Organic Substances Using Oxygen-Consuming Cathodes. U.S. Patent 6,402,930 B1, June 11, 2002.

(6) Deacon, H. Manufacture of Chlorine. U.S. Patent 85,370A, December 29, 1868.

(7) Deacon, H. Improvement in Apparatus for the Manufacture of Chlorine. U.S. Patent 118,209A, Augugust 22, 1871.

(8) Wattimena, F.; Sachtler, W. M. H. M. H. Catalyst Research for the Shell Chlorine Process. *Stud. Surf. Sci. Catal.* **1981**, *7*, 816−827.

(9) Pan, H. Y.; Minet, R. G.; Benson, S. W.; Tsotsis, T. T. Process for Converting Hydrogen Chloride to Chlorine. *Ind. Eng. Chem. Res.* **1994**, *33* (12), 2996−3003.

(10) Hisham, M. W. M.; Benson, S. W. Thermochemistry of the Deacon Process. *J. Phys. Chem.* **1995**, *99* (16), 6194−6198.

(11) Mortensen, M.; Minet, R. G.; Tsotsis, T. T.; Benson, S. W. The Development of a Dual Fluidized-Bed Reactor System for the Conversion of Hydrogen Chloride to Chlorine. *Chem. Eng. Sci.* **1999**, *54* (13−14), 2131−2139.

(12) Kiyoura, T.; Kogure, Y.; Nagayama, T.; Kanaya, K. Manufacturing Process of Chlorine. U.S. Patent 4,822,589, April 18, 1981.

(13) Itoh, H.; Kono, Y.; Ajioka, M.; Takenaka, S.; Kataita, M. Production Process of Chlorine. U.S. Patent 4,803,065, February 7, 1989.

(14) Seki, K. Development of RuO2/Rutile-TiO2 Catalyst for Industrial HCl Oxidation Process. *Catal. Surv. Asia* **2010**, *14* (3), 168−175.

(15) López, N.; Gómez-Segura, J.; Marín, R. P.; Pérez-Ramírez, J. Mechanism of HCl Oxidation (Deacon Process) over RuO2. *J. Catal.* **2008**, *255* (1), 29−39.

(16) Crihan, D.; Knapp, M.; Zweidinger, S.; Lundgren, E.; Weststrate, C. J.; Andersen, J. N.; Seitsonen, A. P.; Over, H. Stable Deacon Process for HCl Oxidation over RuO2. *Angew. Chem., Int. Ed.* **2008**, *47* (11), 2131−2134.

(17) Over, H. Atomic-Scale Understanding of the HCl Oxidation Over RuO2, A Novel Deacon Process. *J. Phys. Chem. C* **2012**, *116* (12), 6779−6792.

(18) Wolf, A.; Kintrup, J.; Schluter, O. F.-K.; Mleczko, L.; Schluter, O. F.-K.; Schubert, S. Processes for the Preparation of Chlorine by Gas Phase Oxidation. U.S. Patent 2007/0292336 A1, December 20, 2007.

DOI: 10.1021/acs.iecr.8b01141
Ind. Eng. Chem. Res. 2018, 57, 7795−7801

(19) Wolf, A.; Mleczko, L.; Schubert, S.; Schluter, O. F.-K. Processes and Apparatus for the Production of Chlorine by Gas Phase Oxidation. U.S. Patent 2007/0274901 A1, November 29, 2007.
(20) Tetsuya, S.; Yasuhiko, M.; Seiji, I. Production of Chlorine. Japan Patent 4192354(B2), October 3, 2008.
(21) Hammes, M.; Valtchev, M.; Roth, M. B.; Stöwe, K.; Maier, W. F. A Search for Alternative Deacon Catalysts. *Appl. Catal., B* **2013**, *132*−*133*, 389−400.
(22) Mondelli, C.; Amrute, A. P.; Schmidt, T.; Pérez-Ramírez, J. A Delafossite-Based Copper Catalyst for Sustainable Cl2 Production by HCl Oxidation. *Chem. Commun.* **2011**, *47* (25), 7173.
(23) Mondelli, C.; Amrute, A. P.; Krumeich, F.; Schmidt, T.; Pérez-Ramírez, J. Shaped RuO2/SnO2-Al2O3 Catalyst for Large-Scale Stable Cl2 Production by HCl Oxidation. *ChemCatChem* **2011**, *3* (4), 657−660.
(24) Iwanaga, K.; Seki, K.; Hibi, T.; Issoh, K.; Suzuta, T.; Nakada, M.; Mori, Y.; Abe, T. *The Development of Improved Hydrogen Chloride Oxidation Process*, R&D Report; Sumitomo Chemical Co., 2004.
(25) Upham, D. C.; Gordon, M. J.; Metiu, H.; McFarland, E. W. Halogen-Mediated Oxidative Dehydrogenation of Propane Using Iodine or Molten Lithium Iodide. *Catal. Lett.* **2016**, *146* (4), 744−754.
(26) Upham, D. C.; Snodgrass, Z. R.; Zavareh, M. T.; McConnaughy, T. B.; Gordon, M. J.; Metiu, H.; McFarland, E. W. Molten Salt Chemical Looping for Reactive Separation of HBr in a Halogen-Based Natural Gas Conversion Process. *Chem. Eng. Sci.* **2017**, *160*, 245−253.
(27) Lovering, D.; Gale, R. *Molten Salt Techniques*; Plenum Press: New York, 1987; Vol. *3*.
(28) Guan, X.; Su, S.; Pal, U. B.; Powell, A. C. Periodic Shorting of SOM Cell to Remove Soluble Magnesium in Molten Flux and Improve Faradaic Efficiency. *Metall. Mater. Trans. B* **2014**, *45* (6), 2138−2144.
(29) Su, S.; Pal, U.; Guan, X. Zero-Direct-Carbon-Emission Aluminum Production by Solid Oxide Membrane-Based Electrolysis Process. In *Advances in Molten Slags, Fluxes, and Salts: Proceedings of the 10th International Conference on Molten Slags, Fluxes and Salts 2016*; Reddy, R. G., Chaubal, P., Pistorius, P. C., Pal, U., Eds.; Springer International Publishing: Cham, 2016; pp 781−790.
(30) Guan, X.; Pal, U. B.; Jiang, Y.; Su, S. Clean Metals Production by Solid Oxide Membrane Electrolysis Process. *J. Sustain. Metall.* **2016**, *2* (2), 152−166.
(31) Su, S.; Pal, U.; Guan, X. Solid Oxide Membrane Electrolysis Process for Aluminum Production: Experiment and Modeling. *J. Electrochem. Soc.* **2017**, *164* (4), F248−F255.
(32) Pal, U.; Su, S.; Villalon, T. Molten Flux Design for Solid Oxide Membrane-Based Electrolysis of Aluminum from Alumina. In *Applications of Process Engineering Principles in Materials Processing, Energy and Environmental Technologies: An EPD Symposium in Honor of Professor Ramana G. Reddy*; Wang, S., Free, M. L., Alam, S., Zhang, M., Taylor, P. R., Eds.; Springer International Publishing: Cham, 2017; pp 35−44.
(33) Lewis, W. K.; Gilliland, E. R.; Hipkin, H. Carbon-Steam Reaction at Low Temperatures. *Ind. Eng. Chem.* **1953**, *45* (8), 1697−1703.
(34) Rao, V.; Datta, R. Development of a Supported Molten-Salt Wacker Catalyst for the Oxidation of Ethylene to Acetaldehyde. *J. Catal.* **1988**, *114* (2), 377−387.
(35) Van Setten, B.; Van Gulijk, C.; Makkee, M.; Moulijn, J. Molten Salts Are Promising Catalysts. How to Apply in Practice? *Top. Catal.* **2001**, *16/17* (1/4), 275−278.
(36) Kumar, C. P.; Gaab, S.; Müller, T. E.; Lercher, J. A. Oxidative Dehydrogenation of Light Alkanes on Supported Molten Alkali Metal Chloride Catalysts. *Top. Catal.* **2008**, *50* (1−4), 156−167.
(37) Allen, J. A. Energetic Criteria for Oxychlorination Catalysts. *J. Appl. Chem.* **1962**, *12* (9), 406−412.
(38) Ruthven, D. M.; Kenney, C. N. The Kinetics of the Oxidation of Hydrogen Chloride over Molten Salt Catalysts. *Chem. Eng. Sci.* **1968**, *23* (9), 981−990.
(39) Ruthven, D. M.; Kenney, C. N. Equilibrium Chlorine Pressures over Cupric Chloride Melts. *J. Inorg. Nucl. Chem.* **1968**, *30* (4), 931−944.
(40) Moroney, L.; Rassias, S.; Roberts, M. W. Chemisorption of HCl and H2S by Cu(111)-O Surfaces. *Surf. Sci.* **1981**, *105* (1), L249−L254.
(41) Roine, A.; Kotiranta, T.; Eerola, H.; Lamberg, P. *HSC Chemistry, Chemical Reaction and Equilibrium Software*, Version 6.0; Qutotec Research Oy: Finland, 2007.
(42) Bian, J.; Wei, X. W.; Jin, Y. R.; Wang, L.; Luan, D. C.; Guan, Z. P. Direct Synthesis of Dimethyl Carbonate over Activated Carbon Supported Cu-Based Catalysts. *Chem. Eng. J.* **2010**, *165* (2), 686−692.
(43) Kim, M. H.; Ham, S.-W.; Lee, J.-B. Oxidation of Gaseous Elemental Mercury by Hydrochloric Acid over CuCl2/TiO2-Based Catalysts in SCR Process. *Appl. Catal., B* **2010**, *99* (1−2), 272−278.
(44) Tomishige, K.; Sakaihori, T.; Sakai, S.-I.; Fujimoto, K. Dimethyl Carbonate Synthesis by Oxidative Carbonylation on Activated Carbon Supported CuCl2 Catalysts: Catalytic Properties and Structural Change. *Appl. Catal., A* **1999**, *181* (1), 95−102.
(45) Muddada, N. B.; Olsbye, U.; Leofanti, G.; Gianolio, D.; Bonino, F.; Bordiga, S.; Fuglerud, T.; Vidotto, S.; Marsella, A.; Lamberti, C. Quantification of Copper Phases, Their Reducibility and Dispersion in Doped-CuCl2/Al2O3 Catalysts for Ethylene Oxychlorination. *Dalt. Trans.* **2010**, *39* (36), 8437.
(46) Zhang, T.; Troll, C.; Rieger, B.; Kintrup, J.; Schlüter, O. F. K.; Weber, R. Composition Optimization of Silica-Supported Copper (II) Chloride Substance for Phosgene Production. *Appl. Catal., A* **2009**, *365* (1), 20−27.
(47) Duke, F. R.; Fleming, R. A. Density and Electrical Conductance in the System KCl-ZnCl2. *J. Electrochem. Soc.* **1957**, *104* (4), 251.
(48) Andreasen, H. A.; Mahan, A.; Bjerrum, N. J. Densities of Molten Potassium Chloride-copper(II) Chloride Obtained by the Automated Float Method. *J. Chem. Eng. Data* **1981**, *26* (2), 195−197.
(49) Ruthven, D. M.; Kenney, C. N. The Kinetics of Oxygen Absorption in Molten Salts Containing Cuprous Chloride. *Chem. Eng. Sci.* **1967**, *22* (12), 1561−1570.
(50) Fujihala, M.; Zheng, X.-G.; Morodomi, H.; Kawae, T.; Watanabe, I. Magnetic Transition in K4Cu4OCl10: A Model System of Three-Dimensional Spin-1/2 Tetrahedra. *Phys. Rev. B: Condens. Matter Mater. Phys.* **2013**, *87* (14), 144425.

DOI: 10.1021/acs.iecr.8b01141
Ind. Eng. Chem. Res. 2018, 57, 7795−7801